

Quantifying the Flexibility From Industrial Steam Systems for Supporting the Power Grid

Xiandong Xu , Member, IEEE, Wenqiang Sun , Muditha Abeysekera, and Meysam Qadrdan , Senior Member, IEEE

Abstract—With more variable and uncertain patterns of electricity production and consumption, the need for flexibility in the power grid is becoming increasingly crucial. Industrial energy systems have the potential to contribute to providing such flexibility. Yet, there is still a lack of effective methods to quantify the magnitude of available flexibility from industrial energy systems that can be optimally dispatched to support the operation of the power grid. This paper studies the flexibility provision from steam systems, which exist in many energy-intensive industries. A generic model of industrial steam systems with turbine-generators is presented to reflect its interactions with the power grid. Then, a hybrid physics-based and data-driven approach is developed to approximate the boundaries of the flexibility domain at different operating conditions of the steam systems. The proposed flexibility quantification method is applied to two real industrial steam systems in a paper mill and a steel mill. The results show that the proposed method can approximate the flexibility boundaries under uncertainty steam states and reflect key factors that affect the boundaries. Also, it is shown that neglecting the limits imposed by the steam network leads to an overestimation of flexibility boundaries at certain operating conditions.

Index Terms—Flexibility, industrial steam systems, modeling, power grid, quantification.

I. INTRODUCTION

THE power grid is experiencing a fundamental shift towards the integration of renewable energy and the electrification of transport and heat sectors [1]. This shift leads to a high degree of mismatch between supply and demand for electricity and necessitates the need for more flexibility [2]. Hereby an individual asset can provide flexibility to the power grid if the generation injection and/or consumption patterns can be modified in reaction to a signal from the power grid [3].

Traditionally, the flexibility is provided by large power stations. Yet, building large power stations requires significant

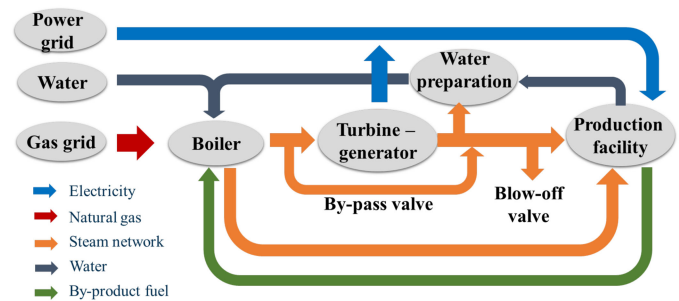


Fig. 1. Schematic diagram of an industrial steam system.

capital costs and has potential environmental impacts. A more economical solution is to look at other sectors, which can support the balancing of electricity supply and demand by changing their electricity generation or consumption [4], [5].

Energy-intensive industries are potential candidates to provide the flexibility [6]. Besides changing the electricity consumption of flexible loads directly [7], another key flexibility source lies in the steam system, which is widely used to drive onsite generations. Most industrial energy users devote significant proportions of their fossil fuel consumption to steam production: pulp and paper (81%), chemicals (42%), petroleum refining (23%), and primary metals (10%) [8]. Fig. 1 shows a typical industrial steam system that is coupled to the power grid via a steam turbine-generator. The steam system can provide flexibility to the power grid by adjusting the steam production of boilers, and the steam flows passing through turbines and valves [9], [10]. By participating in ancillary services markets, industries can realize an additional revenue stream [11]. Industries such as paper mills [12] and steel mills [7] have already been participating in the frequency regulation markets using the flexibility of their onsite generations.

To support facility owners in participating in the ancillary services market, it is necessary to quantify the flexibility that industrial steam systems can provide. Yet, several challenges still need to be addressed.

Firstly, using the steam systems to provide flexibility should not affect industrial processes. Different from thermal power plants, the primary purpose of industrial steam systems is to supply reliable and cost-effective steam to industrial processes. The steam systems couple energy supply systems to industrial processes, i.e. energy demand and by-product fuel production change along with the variations of industrial processes [7], [13]. Although some studies have been conducted considering the

Manuscript received December 29, 2019; revised May 2, 2020; accepted June 28, 2020. Date of publication July 7, 2020; date of current version January 6, 2021. This work was supported in part by the UK Engineering and Physical Sciences Research Council (EPSRC) through MISSION project (EP/S001492/1), the National Natural Science Foundation of China under Grant 51734004, the Fundamental Research Funds for the Central Universities (N2025022), and FLEXIS (Flexible Integrated Energy Systems). FLEXIS is part-funded by the European Regional Development Fund (ERDF), through the Welsh Government. Paper no. TPWRS-01951-2019. (Corresponding author: Meysam Qadrdan.)

Xiandong Xu, Muditha Abeysekera, and Meysam Qadrdan are with the School of Engineering, Cardiff University, Cardiff CF24 3AA, U.K. (e-mail: xux27@cardiff.ac.uk; abeysekeram@cardiff.ac.uk; qadrdanm@cardiff.ac.uk).

Wenqiang Sun is with the Department of Thermal Engineering, Northeastern University, Shenyang 110819, China (e-mail: sunwq@mail.neu.edu.cn).

Color versions of one or more of the figures in this article are available online at <https://ieeexplore.ieee.org>.

Digital Object Identifier 10.1109/TPWRS.2020.3007720

flexibility of onsite generations and electric loads [14], [15], the limits imposed by steam systems on the flexibility have not been well addressed.

Secondly, flexibility metrics of the steam systems need to be characterized according to the requirements of the power grid. From the viewpoint of time scales, the flexibility requirements of the power grid range from milliseconds to years [16]. This paper focuses on the scale from seconds to minutes. At this scale, the key metrics of flexibility can be represented as ramp limit, power capacity, and energy capacity [17], [18]. One way of quantifying these flexibility metrics is to develop a comprehensive model for the concerned system and then using optimization methods to obtain the overall margin for accommodating the variability in the power grid [2]. The weakness of this approach is that the model is difficult to implement for real systems with complex behaviors [19]. The other category of solutions is to characterize the behavior of each component and aggregate the flexibility of the components via geometric approaches. In [20], polytopic feasible sets are employed to aggregate the flexibility of different components. This approach is enhanced in [21] by using zonotopic feasible sets to alleviate the computational challenges. Although the approach is effective in aggregating the flexibility of individual assets, it is not suitable for industrial steam systems as the turbine-generators are interconnected via pipeline networks.

Thirdly, the variations of pressure and temperature of steam lead to changes in enthalpy and affect the electricity outputs of steam turbines. Compared to scheduling based on energy prices described in [24] and [25], providing ancillary services has stricter requirements with respect to the accuracy of adjusting the electricity generation or consumption. Failing to provide services required by the power grid will lead to a significant financial penalty [26]. A commonly used method to deal with decision making under uncertainties is robust optimization [27]. However, the use of robust optimization could lead to over conservative estimation of the available flexibility [28], which will reduce the revenue from providing flexibility. A trade-off between conservatism and maximum flexibility is thus required.

Main works of this paper include: 1) a generic model was presented to describe the interconnections between steam demands, boilers, turbines, and valves in industrial steam systems and their interactions with the electricity system; 2) the flexibility domain of industrial steam systems was characterized accounting for constraint sets of all equipment; 3) a hybrid physics-based and data-driven approach was proposed to estimate the flexibility boundaries considering the variations of temperature and pressure under various operating conditions. The model and the corresponding flexibility quantification method were applied to two real industrial systems.

II. MODELING OF INDUSTRIAL STEAM SYSTEMS

A. System Structure

Fig. 2 shows a typical structure of industrial steam systems. Boilers consume gas or by-product fuel to produce steam. The steam is supplied to a pipeline network with multiple pressure tiers. Steam turbines are installed between different tiers of

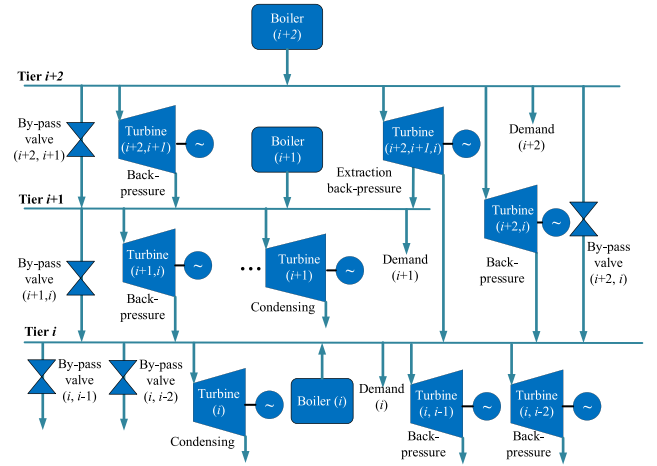


Fig. 2. A typical schematic diagram of industrial steam systems.

the steam network to generate electricity and increase system efficiency. The public power grid meets remaining electricity demand of the industrial site. If the steam flows passing through turbines are not enough to meet the facility's steam demand, additional steam will be supplied via by-pass valves. On the contrary, if more steam is produced than required, the excess steam will be blown off.

B. Assumptions for Steam System Modelling

The following assumptions are made for the modeling of the steam system.

- A1) Equipment at the same tier, such as boilers and turbines, are interconnected via pipelines or valves;
- A2) There is no steam flow from lower pressure tier to higher pressure tier;
- A3) The steam at the outlet of condensing turbines is saturated;
- A4) $\forall i = 1, 2, \dots, n$, where n is the number of pressure tiers in the steam system, the steam can only be injected to tier i from tier $i + 1$ and tier $i + 2$.

These assumptions are usually satisfied by steam systems used in industries, such as integrated pulp and paper mills [24], chemical park [25], ethylene plants [28], and oil refinery [29].

C. System Model

1) *Steam Turbine*: Based on the operational characteristics of industrial steam systems, the extraction back-pressure steam turbine is modeled as two back-pressure steam turbines [28]. Assuming that the turbine is connected to pressure tiers i , $i + 1$, and $i + 2$, the steam passing through the two back-pressure turbines is expressed as $m_{tur}^{i+2, i+1}$ and $m_{tur}^{i+2, i}$, as shown in Fig. 3.

2) *Steam Flow*: The steam flow supplied to tier i is expressed as

$$m_{tier, i}^{in} = \sum_{j=i+1}^{i+2} \left(U_{tur, bp}^{j, i} m_{tur, bp}^{j, i} + m_{by}^{j, i} \right) + U_{boiler}^i m_{boiler}^i \quad (1)$$

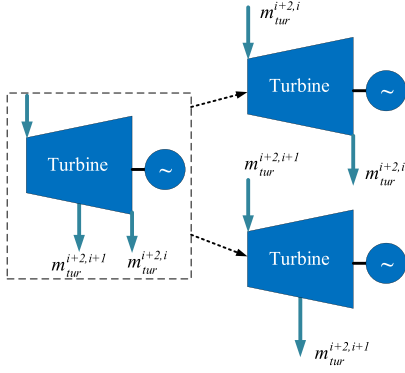


Fig. 3. Equivalent model of the extraction back-pressure steam turbine.

where \mathbf{m}_{boiler}^i is the steam produced by boilers at tier i . \mathbf{U}_{boiler}^i is a 1 by n_{boiler}^i vector of ones. n_{boiler}^i is the number of boilers at tier i . $m_{by}^{j,i}$ is the total steam flow passing through by-pass valves from tier j to tier i . $\mathbf{m}_{tur,bp}^{j,i}$ is the steam flow passing through back-pressure turbines from tier j to tier i . $\mathbf{U}_{tur,bp}^{j,i}$ is a 1 by $n_{tur,bp}^{j,i}$ vector of ones. $n_{tur,bp}^{j,i}$ is the number of back-pressure turbines between tier j and tier i . If $i = n - 1$, then $m_{tier,i}^{in} = \mathbf{U}_{boiler}^i \mathbf{m}_{boiler}^i + m_{by}^{n,n-1} + \mathbf{U}_{tur,bp}^{n,n-1} \mathbf{m}_{tur,bp}^{n,n-1}$. If $i = n$, then $m_{tier,i}^{in} = \mathbf{U}_{boiler}^i \mathbf{m}_{boiler}^i$.

The steam flow supplied by tier i $m_{tier,i}^{out}$ is expressed as

$$m_{tier,i}^{out} = m_{bf}^i + m_d^i + \mathbf{U}_{tur,con}^i \mathbf{m}_{tur,con}^i + \sum_{k=i-2}^{i-1} \left(\mathbf{U}_{tur,bp}^{i,k} \mathbf{m}_{tur,bp}^{i,k} + m_{by}^{i,k} \right) \quad (2)$$

where $\mathbf{m}_{tur,con}^i$ is the steam flow passing through condensing turbines at tier i . $\mathbf{U}_{tur,con}^i$ is a 1 by $n_{tur,con}^i$ vector of ones. $n_{tur,con}^i$ is the number of condensing turbines at tier i . m_d^i is the total steam demand at tier i . m_{bf}^i is the blow-off steam at tier i . If $i = 1$, $m_{tier,i}^{out} = m_{bf}^1 + m_d^1 + \mathbf{U}_{tur,con}^1 \mathbf{m}_{tur,con}^1$. If $i = 2$, $m_{tier,i}^{out} = m_{bf}^2 + m_d^2 + \mathbf{U}_{tur,con}^2 \mathbf{m}_{tur,con}^2 + \mathbf{U}_{tur,bp}^{2,1} \mathbf{m}_{tur,bp}^{2,1} + m_{by}^{2,1}$.

Referring to [31], the steam enthalpy at tier i is estimated by

$$H^i = f_h(p^i, T^i) \quad (3)$$

where p^i is the pressure of steam at tier i . T^i is the temperature of steam at tier i . $f_h : \mathbb{R} \times \mathbb{R} \rightarrow \mathbb{R}$ is a given function.

The enthalpy of the steam at the outlet of condensing turbines at tier i is estimated by

$$H_{sat}^i = f_{h,sat}(p_{sat}^i) \quad (4)$$

where p_{sat}^i is the pressure of saturated steam at tier i . $f_{h,sat} : \mathbb{R} \rightarrow \mathbb{R}$ is a given function.

3) *Gas Consumption*: The total gas consumption of boilers $P_{site}^{in,g}$ is described by

$$P_{site}^{in,g} = \sum_{i=1}^n \mathbf{U}_{boiler}^i (H^i - H_{water}) \mathbf{m}_{boiler}^i / \eta_{boiler}^i \quad (5)$$

where η_{boiler}^i are efficiencies of boilers at tier i . H_{water} is the enthalpy of water supplied to boilers.

4) *Electricity Generation*: The electricity generated by condensing turbines at tier i is expressed as

$$P_{tur,con}^i = \Delta H_{tur,con}^i \eta_{tur,con}^i \mathbf{m}_{tur,con}^i \quad (6)$$

where $\Delta H_{tur,con}^i$ is the enthalpy difference at the inlet and outlet of condensing turbines at tier i , $\Delta H_{tur,con}^i = H^i - H_{sat}^i$. $\eta_{tur,con}^i$ are efficiencies of condensing turbines at tier i .

The electricity generated by back-pressure turbines at tier i is expressed as

$$P_{tur,bp}^i = \sum_{k=i-2}^{i-1} \left(\Delta H_{tur,bp}^{i,k} \eta_{tur,bp}^{i,k} \mathbf{m}_{tur,bp}^{i,k} \right) \quad (7)$$

where $\Delta H_{tur,bp}^{i,k}$ is the enthalpy difference of the inlet and outlet of back-pressure turbines between tier i and tier k , $\Delta H_{tur,bp}^{i,k} = H^i - H^k$. $\eta_{tur,bp}^{i,k} \in \mathbb{R}^{1 \times n_{tur,bp}^{i,k}}$ are efficiencies of back-pressure turbines between tier i and tier k . If $i = 1$, $P_{tur,bp}^i = 0$. If $i = 2$, $P_{tur,bp}^i = \Delta H_{tur,bp}^{2,1} \eta_{tur,bp}^{2,1} \mathbf{m}_{tur,bp}^{2,1}$.

III. QUANTIFICATION OF MAXIMUM FLEXIBILITY FOR SUPPORTING THE POWER GRID

A. Definition of Flexibility

In this paper, the flexibility is defined based on the requirements of ancillary services. A participant has flexibility if it can change its generation/consumption according to a tendered level when instructed. Providing a high magnitude of flexibility services indicates more profits for participants. Yet, the services must be sustained over a period. Hereby, three factors, namely the magnitude of generation regulations, the duration of sustaining the regulations, and ramping limits of the regulations, are considered for describing the flexibility of an industrial steam system.

The magnitude of electricity that the steam system generates during the flexibility provision period is expressed as

$$P_{real} = P_{base} + P_{flexis} \quad (8)$$

where P_{flexis} is the flexibility of the steam system. P_{base} is the generation of the steam system during normal operations. The system is providing upward regulation when $P_{flexis} > 0$, and downward regulation when $P_{flexis} < 0$.

Assume that $F(t)$ is the allowable variation range of P_{flexis} , which also represents the available flexibility for upward regulation and downward regulation, then

$$\forall t \in (t_0, t_0 + t_{min}], [\underline{P}_{flexis}, \bar{P}_{flexis}] \subseteq F(t) \quad (9)$$

where t_0 is the time that a flexibility service is activated. t_{min} is the minimum duration that the service must be sustained. \underline{P}_{flexis} and \bar{P}_{flexis} are the tendered values for downward and upward regulations.

For a given flexibility service, the flexibility provider also needs to ensure that the regulation achieves its required magnitude within the required ramping period. Thus, the flexibility of

the steam system satisfies

$$[\underline{P}_{flexis}, \overline{P}_{flexis}] \subseteq [\underline{R} \times t_{flexis}^{down}, \overline{R} \times t_{flexis}^{up}] \quad (10)$$

where \overline{R} and \underline{R} are the ramp-up and ramp-down rates of electricity generation in the steam system. t_{flexis}^{up} and t_{flexis}^{down} are the time required for the flexibility providers to achieve the tendered upward and downward response.

B. Characterization of Flexibility Domain

The flexibility of a steam system for electricity generation at tier i depends on the constraints sets of turbines (F_{tur}^i), boilers (F_{boiler}^i), by-pass valves (F_{by}^i), and blow-off valves (F_{bf}^i). Thus, the flexibility domain of tier i , F_e^i is expressed as an intersection of these constraint sets as follow

$$\begin{aligned} F_{tur}^i &= \{P_{tur}^i \in \mathbb{R} | \underline{P}_{tur,bp}^i + \underline{P}_{tur,con}^i \\ &\leq P_{tur}^i \leq \overline{P}_{tur,bp}^i + \overline{P}_{tur,con}^i\} \end{aligned} \quad (11)$$

$$\begin{aligned} F_{boiler}^i &= \{\mathbf{m}_{boiler}^i \in \mathbb{R}^{1 \times n_{boiler}^i} | \underline{\mathbf{m}}_{boiler}^i \\ &\leq \mathbf{m}_{boiler}^i \leq \overline{\mathbf{m}}_{boiler}^i\} \end{aligned} \quad (12)$$

$$F_{by}^{i,k} = \{m_{by}^{i,k} \in \mathbb{R}^+ | m_{by}^{i,k} \leq \overline{m}_{by}^{i,k}\} \quad (13)$$

$$F_{bf}^i = \{m_{bf}^i \in \mathbb{R}^+ | m_{bf}^i \leq \overline{m}_{bf}^i\} \quad (14)$$

$$F_e^i = F_{tur}^i \cap F_{boiler}^i \cap F_{by}^i \cap F_{bf}^i \quad (15)$$

where $\underline{P}_{tur,bp}^{i,k}$ and $\overline{P}_{tur,bp}^{i,k}$ are the lower and upper bounds of $P_{tur,bp}^{i,k}$, $\underline{P}_{tur,con}^i$ and $\overline{P}_{tur,con}^i$ are the lower and upper bounds of $P_{tur,con}^i$, $\underline{\mathbf{m}}_{boiler}^i$ and $\overline{\mathbf{m}}_{boiler}^i$ are the lower and upper bounds of steam produced by boilers at tier i . $\overline{m}_{by}^{i,k}$ is the upper bound of the steam passing through by-pass valves between tier i and tier k . \overline{m}_{bf}^i is the upper bound of the blow-off steam at tier i .

Besides real energy consumption, facility owners also need to purchase supply capacities from the public grids based on maximum energy demands. Thus, the flexibility of the steam system is also limited by purchased electricity and gas capacities from the public grids.

The flexibility of import electricity is expressed as

$$F_{site}^{in,e} = \{P_{site}^{in,e} \in \mathbb{R} | \underline{P}_{site}^{in,e} \leq P_{site}^{in,e} \leq \overline{P}_{site}^{in,e}\} \quad (16)$$

where $\overline{P}_{site}^{in,e}$ is the maximum import from the public power grid. $\underline{P}_{site}^{in,e}$ is the limit of feed-in electricity to the public power grid.

The flexibility of import gas is expressed as

$$F_{site}^{in,g} = \{P_{site}^{in,g} \in \mathbb{R}^+ | P_{site}^{in,g} \leq \overline{P}_{site}^{in,g}\} \quad (17)$$

where $\overline{P}_{site}^{in,g}$ is the purchased capacity from the public gas grid.

By aggregating the flexibility of all tiers and constraints of import gas and electricity, the total flexibility of the steam system F_{site} is expressed as

$$F_{site} = F_{site}^{in,e} \cap F_{site}^{in,g} \cap \left(\bigcup_{i=1}^n F_e^i \right) \quad (18)$$

The electricity generation of steam turbines is determined by the steam flow rate and the enthalpy difference between the inlet and outlet of steam turbines. Yet, the enthalpy differences vary as the temperature and pressure of the steam change. To address the variations, a hybrid physics-based and data-driven approach is given in the next subsection.

C. Approximation of Flexibility Domain

In practice, the steam temperature T^i and the steam pressure p^i at tier i are controlled, $\Delta H_{tur,con}^i$ is within the lower bound $\Delta \underline{H}_{tur,con}^i$ and the upper bound $\Delta \overline{H}_{tur,con}^i$

$$\Delta \overline{H}_{tur,con}^i = f_h(\overline{p}^i, \overline{T}^i) - H_{sat}^i \quad (19)$$

$$\Delta \underline{H}_{tur,con}^i = f_h(\underline{p}^i, \underline{T}^i) - H_{sat}^i \quad (20)$$

where \underline{T}^i and \overline{T}^i are the lower and upper operation limits of T^i . \underline{p}^i and \overline{p}^i are the lower and upper operational limits of p^i .

Then $P_{tur,con}^i$ satisfies

$$\overline{P}_{tur,con}^i \geq \overline{P}_{tur,con}^{i,app} = \Delta \underline{H}_{tur,con}^i \eta_{tur,con}^i \overline{\mathbf{m}}_{tur,con}^i \quad (21)$$

$$\underline{P}_{tur,con}^i \leq \underline{P}_{tur,con}^{i,app} = \Delta \overline{H}_{tur,con}^i \eta_{tur,con}^i \underline{\mathbf{m}}_{tur,con}^i \quad (22)$$

where $\underline{\mathbf{m}}_{tur,con}^i$ and $\overline{\mathbf{m}}_{tur,con}^i$ are the lower and upper bounds of steam fed to condensing turbines at tier i .

The enthalpy difference of back-pressure steam turbines between tier i and tier k , namely $\Delta H_{tur,bp}^{i,k}$, is within the lower bound $\Delta \underline{H}_{tur,bp}^{i,k}$ and the upper bound $\Delta \overline{H}_{tur,bp}^{i,k}$

$$\Delta \underline{H}_{tur,bp}^{i,k} = f_h(\underline{p}^i, \underline{T}^i) - f_h(\overline{p}^k, \overline{T}^k) \quad (23)$$

$$\Delta \overline{H}_{tur,bp}^{i,k} = f_h(\overline{p}^i, \overline{T}^i) - f_h(\underline{p}^k, \underline{T}^k) \quad (24)$$

With the approximated enthalpies, $P_{tur,bp}^i$ satisfies

$$\overline{P}_{tur,bp}^i \geq \overline{P}_{tur,bp}^{i,app} = \sum_{k=i-2}^{i-1} \left(\Delta \underline{H}_{tur,bp}^{i,k} \eta_{tur,bp}^{i,k} \overline{\mathbf{m}}_{tur,bp}^{i,k} \right) \quad (25)$$

$$\underline{P}_{tur,bp}^i \leq \underline{P}_{tur,bp}^{i,app} = \sum_{k=i-2}^{i-1} \left(\Delta \overline{H}_{tur,bp}^{i,k} \eta_{tur,bp}^{i,k} \underline{\mathbf{m}}_{tur,bp}^{i,k} \right) \quad (26)$$

where $\underline{\mathbf{m}}_{tur,bp}^{i,k}$ and $\overline{\mathbf{m}}_{tur,bp}^{i,k}$ are the lower and upper bounds of steam fed to back-pressure turbines between tier i and tier k .

A key question in the above estimation is how to identify the bounds of steam enthalpy. Due to friction losses, the pressure level of the steam system drops as the steam demand goes up. On the contrary, due to a higher steam flow velocity, the temperature drop decreases when the steam demand goes up. As a result, the minimum enthalpy in practice is higher than the enthalpy that is calculated using minimum temperature and minimum pressure. Similarly, the maximum enthalpy in practice is lower than the enthalpy that calculated using the maximum temperature and pressure.

To control the degree of conservatism, a data-driven approach is considered based on historical data. The following uncertainty

set is used to represent temperature and pressure.

$$U(T^i, m_{tier,i}^{out}) = \{T^i | T^i = T_{avg}^i + \Delta T^i \cdot z^i, |z^i| \leq \Gamma\} \quad (27)$$

$$U(p^i, m_{tier,i}^{out}) = \{p^i | p^i = p_{avg}^i + \Delta p^i \cdot z^i, |z^i| \leq \Gamma\} \quad (28)$$

where T_{avg}^i and p_{avg}^i represent the average temperature and pressure under the steam demand level $m_{tier,i}^{out}$ at tier i . ΔT^i is the largest possible deviation of T^i . Δp^i is the largest possible deviation of p^i . z^i denotes the extent and direction of parameter deviation, and Γ is an uncertainty budget.

The flexibility domains of various turbines cannot be added up directly, as the steam flows passing through the turbines are interconnected via the steam network. The flexibility boundaries of the steam system across the whole site are formulated as two optimization problems as follows.

The upward flexibility \bar{F}_{site} is expressed as

$$\bar{F}_{site} = \max \sum_{i=1}^n [\bar{P}_{tur,bp}^{i,app} + \bar{P}_{tur,con}^{i,app}] - P_{site}^{gen} \quad (29)$$

s.t.

$$m_{tier,i}^{in} = m_{tier,i}^{out}, \forall i = 1, 2, \dots, n \quad (30)$$

$$P_{site}^d = P_{site}^{gen} + P_{site}^{in,e} \quad (31)$$

(11)–(17), (21), (25), (27)–(28)

where P_{site}^d is the electricity demand of the site. P_{site}^{gen} is the electricity generation of turbine-generators at all tiers, $P_{site}^{gen} = \sum_{i=1}^n (P_{tur,con}^i + P_{tur,bp}^i)$.

The downward flexibility \underline{F}_{site} is expressed as

$$\underline{F}_{site} = \min \sum_{i=1}^n [\underline{P}_{tur,bp}^{i,app} + \underline{P}_{tur,con}^{i,app}] - P_{site}^{gen} \quad (32)$$

s.t.

(11)–(17), (22), (26)–(28), (30)–(31)

For a given flexibility service with ramp periods of t_{flexis}^{up} and t_{flexis}^{down} , the maximum values of flexibility are bounded by

$$\begin{aligned} & [\underline{P}_{tur,con}^{i,app} - P_{tur,con}^i, \bar{P}_{tur,con}^{i,app} - P_{tur,con}^i] \\ & \subseteq [t_{flexis}^{down} \underline{R}_{tur,con}^i, t_{flexis}^{up} \bar{R}_{tur,con}^i] \end{aligned} \quad (33)$$

$$\begin{aligned} & [\underline{P}_{tur,bp}^{i,app} - P_{tur,bp}^i, \bar{P}_{tur,bp}^{i,app} - P_{tur,bp}^i] \\ & \subseteq [t_{flexis}^{down} \underline{R}_{tur,bp}^i, t_{flexis}^{up} \bar{R}_{tur,bp}^i] \end{aligned} \quad (34)$$

where $\underline{R}_{tur,con}^i$ and $\bar{R}_{tur,con}^i$ are ramp-down and ramp-up limits of $P_{tur,con}^i$. $\underline{R}_{tur,bp}^i$ and $\bar{R}_{tur,bp}^i$ are ramp-down and ramp-up limits of $P_{tur,bp}^i$. Note that only the ramp rates of steam turbine generators are considered in this paper, based on the assumption that the line-pack of steam systems in practice can support the gas boilers to follow the adjustment of steam turbines.

IV. CASE STUDIES

The proposed approach for approximating the flexibility boundaries was applied to two real case studies. In case I, an

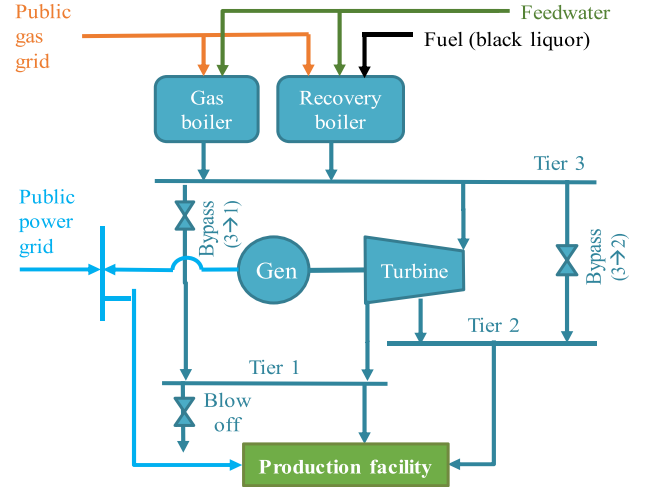


Fig. 4. Schematic diagram of the steam system in case I.

integrated pulp and paper mill with one turbine-generator was studied to quantify its flexibility range at each time step, as well as dispatchable flexibility for a specific ancillary service. In case II, an integrated iron and steel mill with multiple turbine-generators was studied to quantify the impact of different types of steam demands on the flexibility of the still mill. The steam system model and the flexibility quantification approach were implemented in MATLAB 2019b with the support of the X Steam package [31].

A. Case I: An Integrated Pulp and Paper Mill

Fig. 4 presents a schematic diagram of the steam system, which consists of 3 pressure tiers: tier 1 at 3.5 barg; tier 2 at 12barg; and tier 3 at 72 barg. A gas boiler and a recovery boiler are installed at tier 3. The recovery boiler burns by-product fuel, namely black liquor, and natural gas to generate steam. The amount of by-product fuel depends on the production processes, which are considered to be inflexible.

A back-pressure steam turbine with steam extraction at tier 2 produces mechanical energy from the steam expansion process. The steam turbine is coupled to a generator to provide electricity for on-site demands. Any surplus/deficit between the on-site electricity generation and the electricity demand of the site is balanced by the public power grid.

Two by-pass valves are installed to transfer steam between different tiers. These valves are used when the steam turbine is not operational or when the steam demand exceeds the capacity of the steam turbine. A blow-off valve at tier 1 releases any excess steam that is more than the steam required at tier 1.

The feedwater of boilers was assumed to be constant at 104 °C and 100 barg. The LHV of natural gas is 36.67 MJ/Nm³. The LHV of black liquor is 8061 MJ/t. The rated capacity of the steam turbine-generator is 10.5 MW. The ramp rate of the generator is 7% of its rated capacity per minute. Other parameters of the steam system are shown in Table I [32]. Efficiencies of boilers in Table I are based on the LHV of fuels.

TABLE I
PARAMETERS OF THE STEAM SYSTEM IN CASE I

Tier	Equipment	Efficiency	Minimum flow (t/h)	Maximum flow (t/h)
3	Gas boiler	0.93 (Gas to heat)	10	40
	Recovery boiler	0.88 (fuel to heat)	7.5	30
3→2	Steam turbine (extraction)	0.9 (heat to power)	0	10
3→1	Steam turbine (back-pressure)	0.9 (heat to power)	7	70
3→2	By-pass valve 1		0	25
3→1	By-pass valve 2		0	40
1	Blow-off valve		0	50

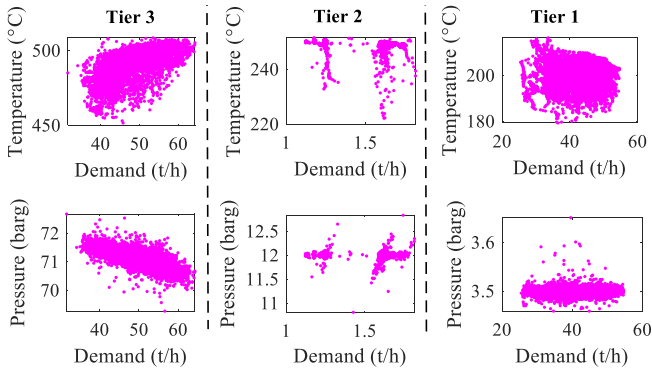


Fig. 5. Historical temperature and pressure data of the steam at all tiers.

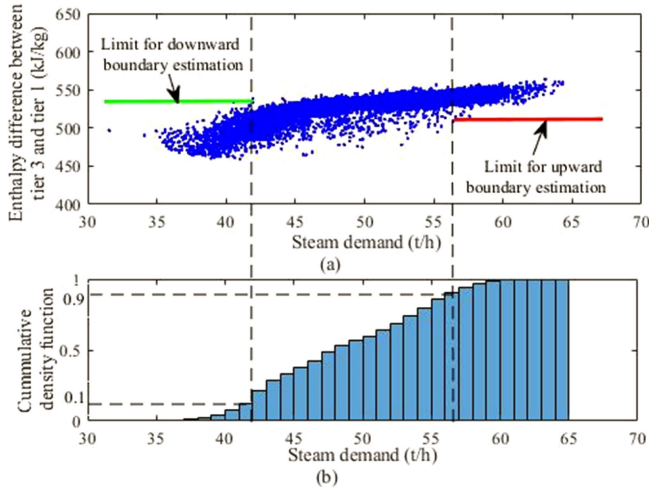


Fig. 6. Variation of steam enthalpy difference between tier 3 and tier 1.

1) *Approximating the Flexibility Boundaries for Upward and Downward Regulations:* Fig. 5 shows the historical data of temperature and pressure of the steam against levels of demand. Based on these data, the variation of enthalpy difference between different tiers against steam demand was acquired as shown in Fig. 6. As the level of steam demand at tier 2 is negligible compared with tier 1 and 3 and no blow-off valve is installed at tier 2, the impact of tier 2 was neglected in this case.

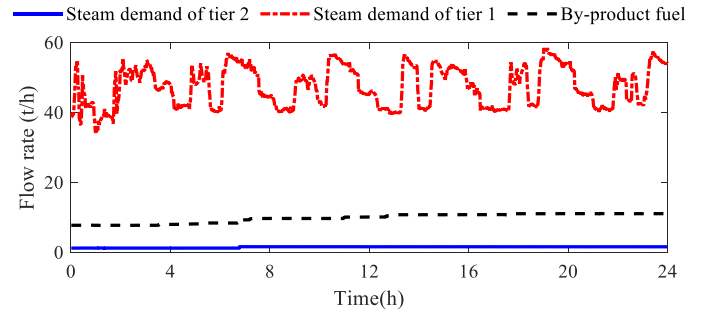


Fig. 7. Flow rates of steam demands and by-product fuel.

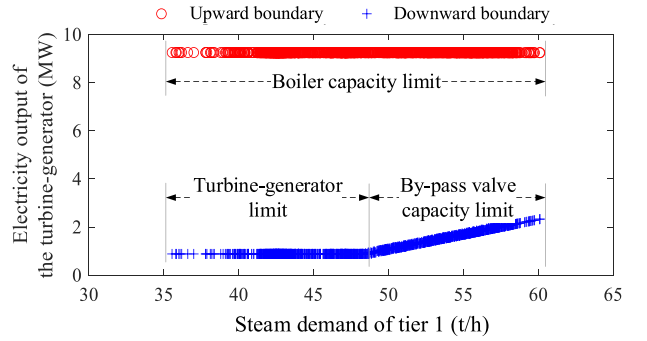


Fig. 8. Minimum and maximum electricity outputs of the turbine-generator under different levels of steam demand.

Due to uncertainties in steam temperature and pressure, the enthalpy difference between tier 3 and tier 1 varies at different demand levels. This variation leads to a different amount of electricity generations under the same steam flow rate. To ensure the security of steam supply to the production facility, an uncertainty budget of 80% was used for approximating upward and downward boundaries. The variation of the enthalpy difference for the upward boundary was approximated by the data set with a cumulative density function (CDF) above 90%. Accordingly, the variation of the enthalpy difference for the downward boundary was approximated by the data set with a CDF below 10%.

For estimating the upward flexibility boundary, the value in the red line in Fig. 6 was used to represent the lower bound of the enthalpy difference in (23). For estimating the downward flexibility boundary, the value in the green line in Fig. 6 was used to represent the upper bound of the enthalpy difference in (24). These two values combined with profiles of the steam demand were used for approximating the flexibility boundaries.

Fig. 7 presents the real operation data of a winter day in 2019, including steam demands at tiers 1 and 3, and the supply flow rate of by-product fuel. The data at one-minute resolution were used to quantify the maximum upward and downward regulations for the electricity output of the turbine-generator.

Fig. 8 shows the boundaries for upward and downward regulations corresponding to different levels of steam demand. The boundaries were used for describing the maximum potential to provide flexibility. As the capacity of the blow-off valve (50t/h) plus the level of steam demand in most historical data is much higher than the total capacity of boilers (30+40t/h), the upward flexibility boundary is determined by capacities of the boilers.

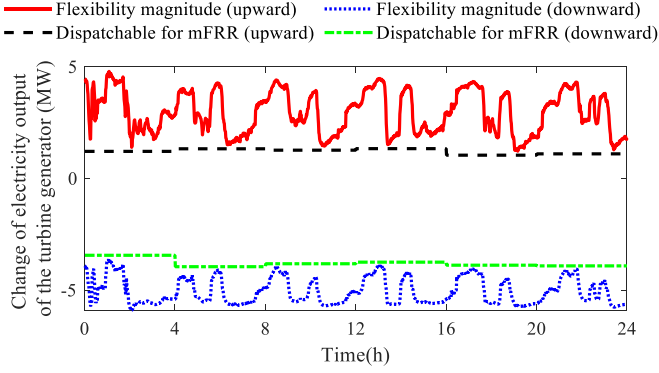


Fig. 9. Variations of flexibility boundaries for mFRR.

The downward boundary includes two segments with different slopes. When the steam demand is below 47.5 t/h, the maximum downward flexibility is limited by the minimum allowable flow rate of the turbine-generator. The magnitude of available flexibility is almost constant. When the steam demand is above 47.5 t/h, the maximum downward flexibility is constrained by rated capacities of by-pass valves and steam demands at tier 1 and tier 2. As capacities of the by-pass valves are fixed, the minimum electricity output of the turbine-generator increases as the steam demand changes.

2) *Quantifying the Flexibility for Ancillary Services:* In this case, the flexibility for the manual Frequency Restoration Reserve (mFRR) in Austria [33] was studied. The facility owner needs to procure the available flexibility in blocks of four hours. The response time for mFRR is 15 min, which indicates that the maximum flexibility magnitude is around 4.7 MW ($0.03 [\% \text{ of the rated capacity per minute}] \times 10.5 [\text{MW rated capacity}] \times 15 [\text{minutes}]$).

Fig. 9 shows the magnitude of flexibility at each time step and the dispatchable flexibility to the grid based on the requirements for mFRR. The magnitude of flexibility was acquired from the operational limits of the turbine-generator in Fig. 8 minus the operating point of the turbine-generator. Due to the change in steam demand, the amount of electricity output from the turbine-generator keeps varying, which leads to different magnitudes of flexibility. To ensure the availability for flexibility provision, the dispatchable flexibility for mFRR was chosen as the minimum magnitudes of the flexibility for the next 4 h (see the dashed black line and the dash-dotted green line in Fig. 9).

Although conducting detailed financial analysis is beyond the scope of this paper, a simple calculation was done to provide an insight into the magnitude of additional revenue that can be realized through providing mFRR service. Based on the dispatchable flexibility shown in Fig. 9, 1 MW was used for mFRR positive (increasing electricity generation) and 3 MW was used for mFRR negative (decreasing electricity generation). The paper mill can acquire €57,258/year for capacity reserve, referring to the pricing scheme of mFRR in Austria, 2019 [34]. If the steam turbine generator is activated for providing mFRR, more profits can be obtained by exchanging energy with the power grid.

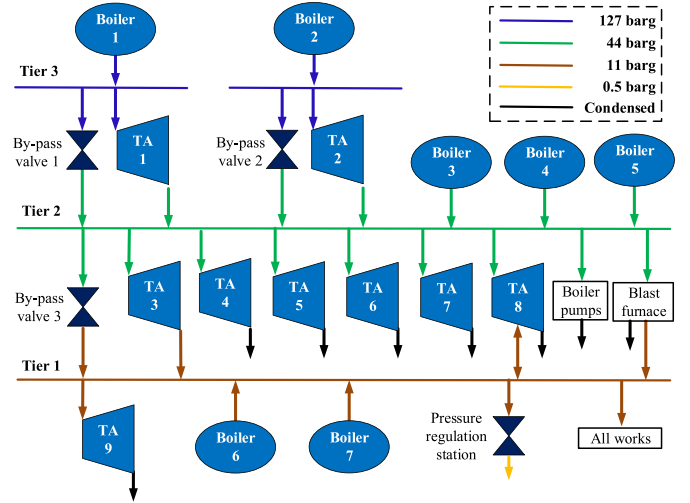


Fig. 10. Schematic diagram of the steam system in case II.

TABLE II
PARAMETERS OF THE STEAM SYSTEM IN CASE II

Tier	Equipment number	Efficiency	Minimum flow (t/h)	Maximum flow (t/h)
3	Boiler 1	0.816	90	157
	Boiler 2	0.865	90	157
	Boiler 3	0.85	18	45
2	Boiler 4	0.699	42	140
	Boiler 5	0.789	45	90
	Boiler 6	0.75	10	65
1	Boiler 7	0.75	10	65
	Turbine 1	0.905	90	176
	Turbine 2	0.9	90	176
3→2	Turbine 3	0.88	50	150
2→1	Turbine 4	0.88	15	80
2	Turbine 5	0.87	15	100
2	Turbine 6	0.885	5	35
2	Turbine 7	0.89	5	32
2	Turbine 8	0.875	45	70
1	Turbine 9	0.85	10	100
3→2	By-pass valve 1		0	157
3→2	By-pass valve 2		0	157
2→1	By-pass valve 3		0	314

B. Case II: Integrated Iron and Steel Mill

Fig. 10 presents a simplified diagram of the steam system of an integrated iron and steel mill, which includes 7 boilers, 9 turbine-alternators (TA), 3 by-pass valves, and steam demands of all the plants. Note that TA8 is an extraction-condensing turbine. When passing through TA8, the steam from Tier 2 will be condensed for electricity generation or extracted to Tier 1. As the pressure level of Tier 1 is higher than the pressure level of TA8's outlet to the condenser, the steam can also go from Tier 1 to TA8 and then be condensed to generate more electricity. The steam system consists of 3 pressure tiers. Parameters of the steam system are shown in Table II. Due to the confidentiality of data, parameters of the steam system were slightly changed. The ramp rate of the turbines was assumed to be 3% of the capacity per minute.

According to (21)–(22), (25)–(26), the flexibility boundaries for upward and downward regulations are relevant to two factors, namely variations of steam enthalpy at different pressures and

TABLE III
PRESSURE AND TEMPERATURE LIMITS OF THE STEAM SYSTEM IN CASE II

Tier	Pressure (barg) Designed (Min/max)	Temperature (°C) Designed (Min/max)
1	11 (10.5/11.5)	320 (320/380)
2	44 (43.5/44.5)	420 (420/438)
3	127 (126.5/127.5)	520 (520/538)

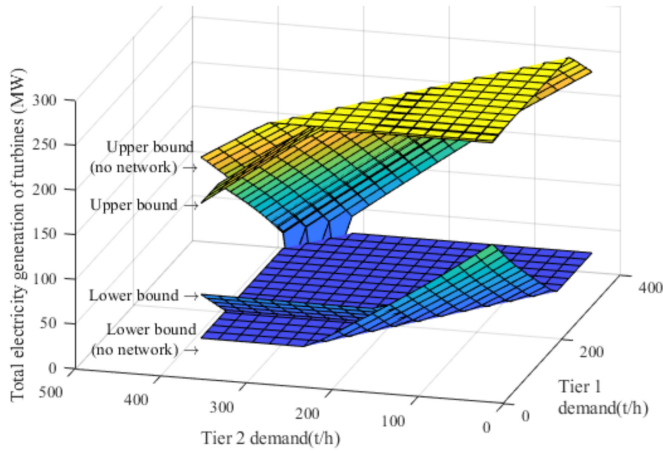


Fig. 11. Flexibility comparison without and with steam transport limits.

temperatures, and the steam flow distribution within the steam system.

In practice, historical data may be confidential or not available to third-party agencies. To support the flexibility quantification, another option is to use operational limits, which could cover the real variation range of the steam states and ensure the security of steam supply to industrial processes. In this case, variations of steam enthalpy were estimated using the limits of temperature and pressure given in Table III. The enthalpy differences of steam at the inlet and output of the turbines were estimated using (19)–(20) for condensing turbines and (23)–(24) for back-pressure turbines.

The steam flow distribution between turbines in Fig. 10 can be adjusted by controlling steam boilers, by-pass valves, and turbines at different tiers. The adjustment would lead to different levels of total electricity output from turbine-generators. In this case, optimization models in (29) and (32) were used to decide the flow rate of steam that could generate the maximum and minimum total electricity output from the whole site. Steam demands were considered as constraints in the optimization models. Specifically, two types of steam demands were studied, namely, 1) steam demands that consume steam, emit water and connect to only one tier; 2) cross-tier steam demand like black furnace fans that consume high-pressure steam and emit low-pressure steam – this was also considered as a steam producer at a lower pressure tier.

Fig. 11 compares the flexibility of the steam turbines with and without considering steam transfer limits. Steam supply and demand need to be balanced at each tier. This balance is achieved by steam transferring through valves and back-pressure turbines. Steam transfer limits result in a smaller range for regulating the electricity output of turbine-generators, compared to the range

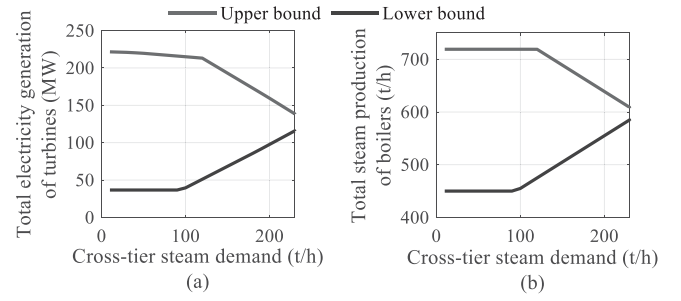


Fig. 12. The impact of cross-tier steam demand on turbine-generation and steam production.

calculated only based on the maximum and minimum steam flow rates passing through turbine-generators.

Fig. 12 shows the total electricity output of turbine-generators and the total steam production of boilers against the cross-tier steam demand between tier 2 and tier 1. For upward regulations, as the cross-tier steam demand increases, the maximum amount of excess steam for increasing electricity generation at tier 2 decreases. Meanwhile, the excess steam at tier 1 increases. However, since the steam in tier 1 has a lower enthalpy than that of tier 2, the maximum electricity generation goes down slightly. Yet, the boundary for downward regulations remains the same as it is determined by the minimum capacity of boilers and turbines.

When the cross-tier steam demand increases beyond ~ 120 t/h, the available capacity of boilers for increasing the electricity generation reaches its limits, and consequently, the flexibility boundary for upward regulations decreases significantly. The flexibility boundary for downward regulation increases (i.e. less downward flexibility) as the excess steam supply at tier 1 needs to be emitted by turbine TA9, which limits its minimum electricity generation.

By providing flexibility services, the steel mill will acquire profits from the power grid. Using the FFR in Great Britain as an example, a tendered price of availability fee was 51.7 £/h for a capacity of 3.2 MW for primary frequency response and 8 MW for secondary and high-frequency response from 08/01/2019 to 08/31/2019 [35]. The tendered duration for each day was 16 h. As shown in Fig. 12(a), the maximum flexibility of the still mill ranges from 5 MW to 80 MW at different levels of cross-tier steam demand. Assume that the same capacities and pricing scheme were applied for the FFR, then the steel mill would receive an estimated payment of £302k/year as the availability fee.

V. CONCLUSION

A flexibility quantification method for industrial steam systems was developed to allow facility owners to estimate their capabilities for providing ancillary services to the power grid. The method provides boundaries to operators for supporting the dispatch of the integrated steam and energy system. The approximated boundaries ensure that providing flexibility to the power grid would not affect the energy supply to industrial processes.

A general model of the steam system connected to gas and electricity systems was developed and applied to the flexibility quantification of two real steam systems. Case studies show that the approximated flexibility boundaries can support operators in estimating the available flexibility for given ancillary services and potential profits from the relevant markets. Also, the results show that neglecting the limits of the steam system will lead to an overestimation of the flexibility boundaries. For large-scale steam systems, the line-pack could accommodate the uncertainty in steam demands and increase the flexibility of the steam generation system. Moreover, some industrial sites have steam accumulators installed, which could further increase the flexibility. These two aspects will be studied in future work.

ACKNOWLEDGMENT

The authors also would like to thank Mr Karl Rittmannsberger from Mondi Group and Dr Chris Williams from Tata Steel Port Talbot for supporting the case studies.

REFERENCES

- [1] Parliamentary Office of Science and Technology, House of Parliament. "Flexible electricity systems". Sep. 2018, [Online]. Available: <https://researchbriefings.parliament.uk/ResearchBriefing/Summary/POST-PN-0587>. Accessed on: Jun. 20, 2019.
- [2] J. Zhao, T. Zheng T, and E. Litvinov, "A unified framework for defining and measuring flexibility in power system," *IEEE Trans Power Syst.*, vol. 31, no. 1, pp. 339–347, Jan. 2015.
- [3] The Office of Gas and Electricity Markets (Ofgem), "Electricity system flexibility," [Online]. Available: <https://www.ofgem.gov.uk/electricity/retail-market/market-review-and-reform/smarter-markets-programme/electricity-system-flexibility>. Accessed: Jun. 14, 2019.
- [4] K. Witkowski, P. Haering, S. Seidelt, and N. Pini, "Role of thermal technologies for enhancing flexibility in multi-energy systems through sector coupling: technical suitability and expected developments," *IET Energy Syst. Integration*, vol. 2, no. 2, pp. 69–79, Mar. 2020.
- [5] M. Cheng, J. Wu, S. J. Galsworthy, C. E. Ugalde-Loo, N. Gargov, and N. Jenkins, "Power system frequency response from the control of Bitumen tanks," *IEEE Trans. Power Syst.*, vol. 31, no. 3, pp. 1769–1778, Jun. 2015.
- [6] W. Sun, Q. Wang, Y. Zhou, and J. Wu, "Material and energy flows of the iron and steel industry: Status quo, challenges and perspectives," *Appl. Energy*, vol. 268, Jun. 15, 2020, Art. no. 114946.
- [7] X. Zhang, G. Hug, J. Z. Kolter, and I. Harjunkoski, "Demand response of ancillary service from industrial loads coordinated with energy storage," *IEEE Trans. Power Syst.*, vol. 33, no. 1, pp. 951–961, May 2017.
- [8] D. Einstein, E. Worrell, and M. Khrushch, "Steam systems in industry: Energy use and energy efficiency improvement potentials," in *Proc. Lawrence Berkeley Nat. Lab.*, Jul. 2001.
- [9] X. Luo, B. Zhang, Y. Chen, and S. Mo, "Modeling and optimization of a utility system containing multiple extractions steam turbines," *Energy*, vol. 36, no. 5, pp. 3501–3512, May 2011.
- [10] J. Qian *et al.*, "Flow rate analysis of compressible superheated steam through pressure reducing valves," *Energy*, vol. 135, pp. 650–658, Sep. 2017.
- [11] A. W. Dowling and V. M. Zavala, "Economic opportunities for industrial systems from frequency regulation markets," *Comp. Chem. Eng.*, vol. 114, pp. 254–264, Jun. 2018.
- [12] P. Hult, "The potential for frequency control in paper mills," M. S. thesis, Dept. Heat Power, Chalmers Univ. Technol., Gothenburg, Sweden, 2015.
- [13] W. Sun, Z. Wang, and Q. Wang, "Hybrid event-, mechanism-and data-driven prediction of blast furnace gas generation," *Energy*, vol. 199, May 2020, Art. no. 117497.
- [14] M. Coatalem, V. Mazauric, C. Le Pape-Gardeux, and N. Maïzi, "Optimizing industries' power generation assets on the electricity markets," *Appl. Energy*, vol. 185, pp. 1744–1756, Jan. 2017.
- [15] F. Angizeh, M. Parvania, M. Fotuhi-Firuzabad, and A. Rajabi-Ghahnavieh, "Flexibility scheduling for large customers," *IEEE Trans Smart Grid*, vol. 10, no. 1, pp. 371–379, Jan. 2019.

- [16] T. Heggarty, J.-Y. Bourmaud, R. Girard, and G. Kariniotakis, "Multi-temporal assessment of power system flexibility requirement," *Appl. Energy*, vol. 238, pp. 1327–1336, Mar. 2019.
- [17] A. Ulbig and G. Andersson, "Analyzing operational flexibility of electric power systems," *Int. J. Elect. Power Energy Syst.*, vol. 72, pp. 155–164, 2015.
- [18] B. Mohandes, M. S. E. Moursi, N. Hatziargyriou, and S. E. Khatib, "A review of power system flexibility with high penetration of renewables," *IEEE Trans Power Syst.*, vol. 34, no. 4, pp. 3140–3155, Jul. 2019.
- [19] Q. Wang and B. Hodge, "Enhancing power system operational flexibility with flexible ramping products: A review," *IEEE Trans. Ind. Inform.*, vol. 13, no. 4, pp. 1652–1664, Aug. 2017.
- [20] L. Zhao, W. Zhang, H. Hao, and K. Kalsi, "A geometric approach to aggregate flexibility modeling of thermostatically controlled loads," *IEEE Trans. Power Syst.*, vol. 32, no. 6, pp. 4721–4731, Nov. 2017.
- [21] F. L. Müller, J. Szabó, O. Sundström, and J. Lygeros, "Aggregation and disaggregation of energetic flexibility from distributed energy resources," *IEEE Trans. Smart Grid*, vol. 10, no. 2, pp. 1205–1214, Mar. 2019.
- [22] H. Nosair and F. Bouffard, "Flexibility envelopes for power system operational planning," *IEEE Trans. Sustain. Energy*, vol. 6, no. 3, pp. 800–809, Apr. 2015.
- [23] B. Botros and J. Brisson, "Targeting the optimum steam system for power generation with increased flexibility in the steam power island design," *Energy*, vol. 36, no. 8, pp. 4625–4632, Aug. 2011.
- [24] D. J. Marshman, T. Chmelyk, M. S. Sidhu, and R. B. Gopaluni, "Energy optimization in a pulp and paper mill cogeneration facility," *Appl. Energy*, vol. 87, no. 11, pp. 3514–3525, Nov. 2010.
- [25] S. Mitra, L. Sun, and I. E. Grossmann, "Optimal scheduling of industrial combined heat and power plants under time-sensitive electricity prices," *Energy*, vol. 54, pp. 194–211, Jun. 2013.
- [26] National Grid. "Firm frequency response (FFR) interactive guidance," 2017. [Online]. Available: <https://www.nationalgrideso.com/balancing-services/frequency-response-services/firm-frequency-response-ffr>. Accessed: Oct. 27, 2019.
- [27] I. E. Grossmann, R. M. Apap, B. A. Calfa, P. García-Herreros, and Q. Zhang, "Recent advances in mathematical programming techniques for the optimization of process systems under uncertainty," *Comput Chem Eng*, vol. 91, pp. 3–14, Jun. 2015.
- [28] F. Shen, L. Zhao, W. Du, W. Zhong, and F. Qian, "Large-scale industrial energy systems optimization under uncertainty: A data-driven robust optimization approach," *Appl. Energy*, vol. 259, Feb. 2020, Art. no. 114199.
- [29] S. R. Micheletto, M. C. Carvalho, and J. M. Pinto, "Operational optimization of the utility system of an oil refinery," *Comput Chem Eng*, vol. 32, no. 1–2, pp. 170–185, Jan. 2008.
- [30] D. Bertsimas and M. Sim. The price of robustness. *Oper. Res.*, vol. 52, no. 1, pp. 35–53, Feb. 2004.
- [31] M. Holmgren. X Steam for Matlab. [Online]. Available: www.x-eng.com. Accessed: Aug. 10, 2019.
- [32] X. Xu *et al.*, "Quantifying flexibility of industrial steam systems for ancillary services: A case study of an integrated pulp and paper mill," *IET Energy Syst. Integration*, vol. 2, no. 2, pp. 124–132, 2020.
- [33] Austrian Power Grid, "Tenders for mFRR in the APG control area". 2019. [Online]. Available: <https://www.apg.at/en/markt/netzregelung/tertiaerregelung/ausschreibungen>. Accessed: Dec. 1, 2019.
- [34] Austrian Power Grid. "Preisentwicklung Regelreservemarkt von KW1 2018 bis KW44." 2019. [Online]. Available: <https://www.apg.at/markt/-/media/92990D10C93746C58DFE8267B1127308.pdf>. Accessed: Dec. 1, 2019.
- [35] National Grid. Post Tender Report - TR15. Jul. 2019. [Online]. Available: <https://www.nationalgrideso.com/document/148226/download>. Accessed: Dec. 8, 2019.
- [36] X. Luo, B. Zhang, Y. Chen, and S. Mo, "Operational planning optimization of multiple interconnected steam power plants considering environmental costs," *Energy*, vol. 37, no. 1, pp. 549–561, Jan. 2012.



Xiandong Xu (Member, IEEE) received the B.Sc. and Ph.D. degrees in electrical engineering from Tianjin University, China, in 2009 and 2015, respectively. He is currently a Research Associate at Cardiff University. His research focuses on modelling and optimization of integrated energy systems, and operational flexibility of heat and industrial sectors.



Wenqiang Sun received the B.Sc. degree in energy and power engineering from Northeastern University, China, the M.Sc. and Ph.D. degrees in thermal engineering from Northeastern University, China, in 2007, 2009, and 2014, respectively.

Currently, he is an Associate Professor at Northeastern University, China. His research interests include energy conversion, waste heat recovery and industrial energy system optimization.



Meysam Qadrdan (Senior Member, IEEE) received the B.Sc. degree in physics from the Ferdowsi University of Mashhad, Iran, the M.Sc. degree in energy systems Engineering from the Sharif University of Technology, Iran, and the Ph.D. degree in electrical engineering from Cardiff University, U.K., in 2005, 2008, and 2012, respectively. Currently, he is a Reader at Cardiff University. His research looks at modelling and optimization of integrated energy systems including electricity, gas and heat.



Muditha Abeysekera received the B.Sc. degree in mechanical engineering from the University of Peradeniya-Sri Lanka (2010), the M.Sc. degree in sustainable energy engineering from the Royal Institute of Technology, Sweden and Universitat Politècnica de Catalunya– Barcelona, Spain (2012) and the Ph.D. degree in electrical engineering from Cardiff University, U.K. (2017).

He is currently a Lecturer at Cardiff University. His research interests are on the design and optimization of multi-energy system infrastructure, the study of

whole system impact of local energy systems and the decarbonization of the UK heat sector.